

Interfacial solvation can explain attraction between like-charged objects in aqueous solution

Cite as: J. Chem. Phys. 152, 104713 (2020); doi: 10.1063/1.5141346

Submitted: 4 December 2019 • Accepted: 4 February 2020 •

Published Online: 13 March 2020



View Online



Export Citation



CrossMark

Alžbeta Kubincová,¹  Philippe H. Hünenberger,¹  and Madhavi Krishnan^{2,a} 

AFFILIATIONS

¹Laboratory of Physical Chemistry, Department of Chemistry and Applied Biosciences, ETH Zurich, Vladimir-Prelog-Weg 2, CH-8093 Zürich, Switzerland

²Physical and Theoretical Chemistry Laboratory, Department of Chemistry, University of Oxford, South Parks Road, Oxford OX1 3QZ, United Kingdom

^aAuthor to whom correspondence should be addressed: madhavi.krishnan@chem.ox.ac.uk

ABSTRACT

Over the past few decades, the experimental literature has consistently reported observations of attraction between like-charged colloidal particles and macromolecules in aqueous solution. Examples include nucleic acids and colloidal particles in the bulk solution and under confinement, and biological liquid–liquid phase separation. This observation is at odds with the intuitive expectation of an interparticle repulsion that decays monotonically with distance. Although attraction between like-charged particles can be rationalized theoretically in the strong-coupling regime, e.g., in the presence of multivalent counterions, recurring accounts of long-range attraction in aqueous solution containing monovalent ions at low ionic strength have posed an open conundrum. Here, we show that the behavior of molecular water at an interface—traditionally disregarded in the continuum electrostatics picture—provides a mechanism to explain the attraction between like-charged objects in a broad spectrum of experiments. This basic principle will have important ramifications in the ongoing quest to better understand intermolecular interactions in solution.

Published under license by AIP Publishing. <https://doi.org/10.1063/1.5141346>

I. INTRODUCTION

Water is an asymmetric molecule with a strong permanent dipole whose response to an electric field gives the bulk fluid its characteristically high relative dielectric permittivity of about 80. In the absence of an external field, random thermal reorientation causes the molecular dipole moment to average out to zero, resulting in no net polarization. However, at an interface in solution, e.g., a cavity, neutral molecule, or macroscopic surface, the hydrogen-bonding symmetry is broken, and molecular water is no longer isotropically oriented. In fact, this broken symmetry in interfacial orientation is not limited to water and represents a general phenomenon related to the charge-shape asymmetry of the molecule.¹ For water, the bent-core molecular structure and the resulting orientational preference at an interface are commonly invoked to explain thermodynamic phenomena such as the preferential hydration of anions compared to cations,¹ ion specific effects on surface tension,² reduced hydration repulsion between surfaces,³ and crystallization of charged

nanoparticles.⁴ Focusing on the interaction between a pair of objects in solution, it seems plausible that any distance-dependent alteration in the orientational behavior of interfacial solvent molecules could be accompanied by a substantial free energy contribution to the potential of mean force. Such a contribution is not accounted for within the framework of continuum-electrostatics theory, which regards the solvent as a smooth, featureless medium, and could carry profound implications for the interpretation of experimental observations.

II. CONTINUUM ELECTROSTATICS MODEL FOR THE INTERACTION BETWEEN LIKE-CHARGED PARTICLES IN SOLUTION

We consider the interaction of two identical like-charged spheres in an aqueous electrolyte containing exclusively monovalent salt at low ionic strength. In low concentrations of monovalent

salt (<1 mM), Poisson–Boltzmann (PB) theory provides an accurate description of electrostatic interactions, and generally predicts a monotonically increasing repulsion with decreasing interparticle separation.^{5,6} Over the past few decades, however, several independent studies have reported long-range attractive interactions between like-charged dielectric particles in low ionic strength solution that depart qualitatively from the PB picture.^{7–19} Note that, under the relevant experimental conditions, corrections such as those arising from ion correlations, finite ion size, and charge density fluctuations are not sufficient to render the screened repulsion attractive at long range.^{20–22} Although some of the experimental reports have come under scrutiny for measurement artifacts,²³ the overall observation has thus far evaded satisfactory explanation and continues to attract theoretical interest.²⁴

To understand how the properties of interfacial water molecules and the associated free-energy change may induce a long-range attraction between like-charged particles, it is necessary to consider the mechanism of charge regulation. Electrical charge on an object in solution generally arises due to ionizable chemical groups via an associative or a dissociative mechanism. For example, acidic groups dissociate to produce an anion and a free proton via the equilibrium reaction $\text{HA} \rightleftharpoons \text{H}^+ + \text{A}^-$ which is governed by an equilibrium constant of dissociation, K and the pH in bulk solution. pK , the negative decadic logarithm of K , is directly related to the free-energy change of the ionization process, and includes a gas-phase component along with the solvation free energies of the reactants and products.²⁵ For particles carrying ionizable surface groups at a number density, Γ , the net electrical charge density as a function of position \mathbf{R} on the particle surface is given by

$$\sigma(\mathbf{R}) = z\alpha(\mathbf{R})\Gamma e, \quad (1)$$

where $z = \pm 1$ denotes the sign of the charge of the ionized group (e.g., $z = -1$ for an acidic group) and e is the elementary charge. In this equation, $\alpha(\mathbf{R})$ is the ionization probability and is given by^{26,27}

$$\alpha(\mathbf{R}) = \frac{1}{1 + 10^{z(\text{pH}-\text{pK})} \exp(z\psi_s(\mathbf{R}))}, \quad (2)$$

where $\psi_s(\mathbf{R})$ represents the value of the dimensionless electrical potential, $\psi(\mathbf{R}) = \frac{e\phi(\mathbf{R})}{k_B T}$, at the surface of the particle, and the energy scale $k_B T$ is the product of Boltzmann's constant and the absolute temperature, T . In this equation, originally proposed by Ninham and Parsegian,²⁶ the pK value is that of the surface ionizable groups. This value need not be identical to the pK value of an isolated ionizable group in bulk solution as the energetics of charging at an interface can be very different than that in free solution.^{25,28} Qualitatively, the pK of an interfacial ionizable group would be expected to shift upwards for an acidic group and downwards for a basic group relative to the value for an isolated group in bulk solution.

Equation (1) serves as the boundary condition for the charge density at the particle surface, where the electrical potential that develops in the electrolyte bulk is determined as a function of position, \mathbf{r} by the non-linear PB equation: $\nabla^2\psi(\mathbf{r}) = \kappa^2 \sinh\psi(\mathbf{r})$. Here, $\kappa = \sqrt{\frac{2e^2c_0}{\epsilon\epsilon_0 k_B T}}$ is the inverse of the Debye length – a measure of the distance over which the electrical potential decays from its surface value, ψ_s due to screening by the cloud of oppositely charged

counterions in solution, ϵ is the relative permittivity of the electrolyte medium ($\epsilon = 78.5$ for water at room temperature), and ϵ_0 is the permittivity of free space. Thus, the ionization state of the surface groups is indirectly also coupled to the salt concentration, c_0 in solution. This study deals with interparticle interactions measured in deionized water of resistivity 18 MΩcm, containing dissolved CO₂ from ambient air, which results in Debye screening lengths, $\kappa^{-1} \sim 100$ nm.

It is evident from Eq. (2) that with the pK and pH held constant, a change in the magnitude of the electrical potential, ψ_s alters the value of the local surface charge. This is exactly what happens when two charged objects approach one another. At a distance of a few Debye lengths, each surface is subjected to the decaying tail of the electrical potential due to the approaching object. For like-charged entities, the magnitude of the surface potential on both particles increases while that of the surface charge decreases, in accord with Eq. (2). This well-established phenomenon is referred to as “charge regulation,” and the electrostatic free energy of the regulated interaction is generally smaller in magnitude than that for surfaces interacting at constant charge.²⁹ However, for all practical purposes, the interaction remains monotonically repulsive as long as the particles carry some non-vanishing electrical charge.³⁰

III. EXCESS HYDRATION FREE ENERGY OF AN INTERFACE BASED ON MOLECULAR SIMULATIONS

Molecular Dynamics (MD) studies on neutral cavities in water have shown that interfacial molecules do not orient isotropically as in the bulk, but rather exhibit a slight preferential orientation of the negative oxygen atom toward the cavity surface.¹ As illustrated in Fig. 1, the effects of introducing a progressively increasing positive or a negative charge in the cavity are qualitatively different. As a neutral cavity acquires an increasing positive charge, the local electric field reinforces the alignment of the interfacial molecules, i.e., strengthens the preferential orientation of the oxygen atoms toward the surface. In contrast, when the cavity acquires an increasing negative charge, the negative oxygen atoms are repelled. The preferential orientation trend observed at the neutral cavity initially weakens, and then inverts: the water molecules flip around, going through a vanishing preferential orientation at some critical value of negative charge. Beyond this point, the positive hydrogen atoms point preferentially toward the cavity surface, and this trend in orientation is reinforced as the magnitude of the negative charge further increases. Similar observations have been made in simulation studies involving planar interfaces.^{2,3,31,32}

In order to quantify the free energy of interfacial water at a charge-regulating surface, we performed MD simulations of pure water at a planar interface. We set up a parallel plate capacitor composed of two walls of area 100 nm² carrying electrical charge of equal magnitude but opposite sign, separated by a gap of about 4 nm [Fig. 2(a)]. The walls consisted of fixed hexagonally packed non-polar and non-hydrogen-bonding atoms of the size of the oxygen atom. The gap was filled with 12 448 simple point charge (SPC) water molecules. Atoms at the surface of each wall are assigned a charge of either 0 or $\pm 1 e$ so as to attain final charge densities of $+|\sigma|$ and $-|\sigma|$ at the left and right plates, respectively. Polarization profiles, $P(z)$ as a function of the distance z from the positive plate were calculated based on 5 ns simulations for different values of $|\sigma|$ [Fig. 2(b)].

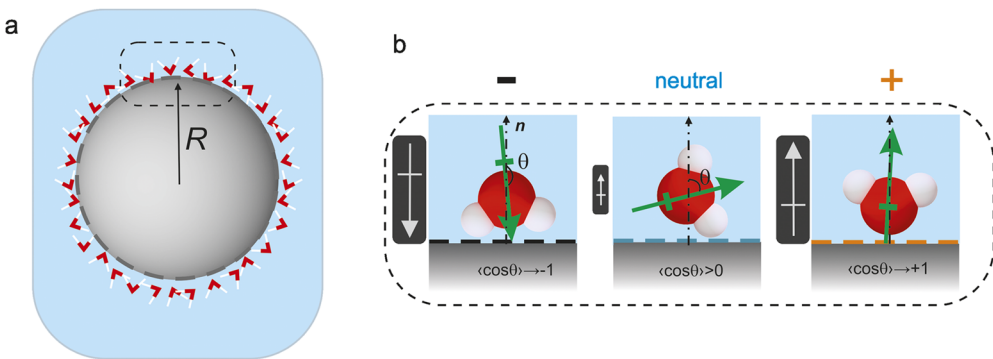


FIG. 1. Molecular water at a charged interface. (a) Schematic depiction of water molecules at the interface between a particle of radius, R and aqueous solution. (b) Configurations illustrative of the average orientation of interfacial water molecules at surfaces that carry a strongly negative charge (left), no charge (center), or a strongly positive charge (right). θ denotes the angle included between the molecular dipole moment (green) and the outward-directed surface normal, n (dashed line). The molecular orientation is inferred from Molecular Dynamics (MD) simulations [Fig. 2(b)], with $\cos\theta$ large and negative ($\rightarrow -1$) for the strongly negative surface, large and positive ($\rightarrow +1$) for the strongly positive surface, and slightly positive (>0) for the neutral surface. As the surface charge changes from zero to strongly negative there is an inversion in the average orientation of interfacial water.

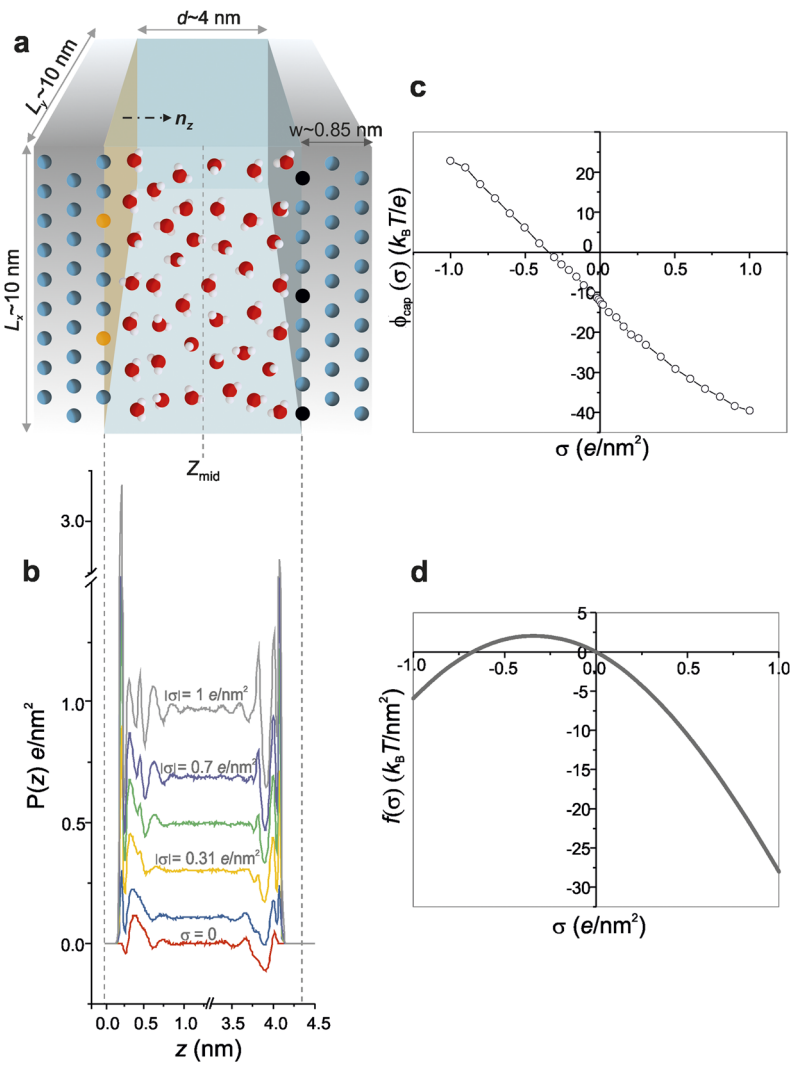


FIG. 2. Excess hydration free energy of a charged interface based on molecular simulations. (a) Schematic representation of the simulated system. The $10 \times 10 nm^2$ parallel-plate capacitor is made up of a positive (left) and negative (right) plate, each composed of three layers of atoms, separated by a gap of about 4 nm filled with water molecules. Interfacial wall atoms carry a charge of 0 or $\pm 1 e$ to attain an overall charge density of $\pm 1 e/nm^2$. The arrow depicts the axis, n_z . (b) The area-averaged profile, $P(z)$ of the polarization projected along the z -axis is extracted from the simulation. Note that the projection along n_z corresponds to a projection along the outward-directed surface normal n for the left plate [i.e., as in Fig. 1(b)], but an inward-directed normal $-n$ for the right plate [i.e., opposite to Fig. 1(b)]. Within about 0.5 nm from the surfaces, the $P(z)$ profiles differ substantially from the bulk value. (c) The electrical potential, $\phi_{cap}(\sigma)$ at the walls as a function of σ is derived from $P(z)$ by integration from the reference position, z_{mid} as described further in the text. (d) Based on the $\phi_{cap}(\sigma)$ curves, the excess hydration free energy per unit area, $f(\sigma)$ is derived by integration over σ (see supplementary material Sec. 1).

We note that within a region of about 0.5 nm from each surface, the polarization departs substantially from the value $\frac{\epsilon-1}{\epsilon}\sigma$ expected for an ideal dielectric medium of relative permittivity ϵ . In order to quantify the excess hydration free energy, i.e., the free energy associated with this extra non-dielectric polarization component, the continuum value was subtracted from $P(z)$, and the resulting function was integrated from a reference position at the midplane of the capacitor, z_{mid} , up to the surface of each plate [Fig. 2(a), supplementary material Sec. I]. This yields the excess electrical potential, ϕ_{cap} at the surface of each plate as a function of charge density, σ [Fig. 2(c)]. A charging integral of the form $f(\sigma) = \int_0^\sigma \phi_{\text{cap}}(\sigma)d\sigma$ then gives the excess hydration free energy per unit area due to the excess polarization as a function of σ [Fig. 2(d)]. The form of $f(\sigma)$ agrees with the qualitative considerations presented in the context of Fig. 1. For a positively charged surface, $f(\sigma)$ decreases monotonically with increasing charge density. In contrast, for a negative surface, $f(\sigma)$ is a non-monotonic function of σ , $f(\sigma)$ increases from $\sigma = 0$, goes through a maximum at $\sigma \approx -0.3 \text{ e/nm}^2$, and decreases thereafter.

This reorientation effect for negative surfaces is also supported by independent experimental evidence. The orientation of water at charged interfaces has been extensively studied using non-linear optical spectroscopy³³ on various types of surfaces, e.g., silica, alumina, positive and negative lipid bilayers. These studies have shown that water molecules are strongly oriented at charged interfaces due to charge–dipole interactions, whereas they are only weakly oriented at neutral surfaces.^{34–38} Importantly, sum-frequency generation vibrational spectroscopy on negatively charged silica surfaces in water have demonstrated that not only is molecular orientation at an interface a function of surface charge density but that water molecules indeed flip around with increasing pH^{36,37,39–41}—which corresponds to increasing negative charge—in line with the behavior suggested by MD simulations (Figs. 1 and 2).

IV. A MODEL OF INTERPARTICLE INTERACTIONS INCLUDING THE EXCESS HYDRATION FREE ENERGY OF THE INTERFACE FROM MOLECULAR SIMULATIONS

We now incorporate the results from molecular simulations into a calculation of the potential of mean force for the interaction of two spherical particles in solution. We represent the total free energy as

$$\Delta F_{\text{tot}}(x) = \Delta F_{\text{el}}(x) + \Delta F_{\text{int}}(x), \quad (3)$$

where x is the inter-surface separation between the particles and each term denotes a free-energy difference with reference to the zero-point set at infinite separation [Fig. 3(a)]. We solve the PB equation for the electrical potential, $\psi(r;x)$ in the electrolyte region between two particles of radius R at a variable separation x , using Eq. (1) as the boundary condition on the surfaces of both spheres. The computation is performed using COMSOL Multiphysics as described in previous work.^{42,43} Note that when solving the PB equation for this system, we neglect the effect of the dielectric interior of the spheres as the corresponding field energy makes a negligible contribution to the overall free energy.⁴² For a charge regulating pair of identical spheres, the charge density, σ , on both spheres decreases upon approach, giving an attractive contribution to the total free

energy that scales as σ^2 with decreasing separation. A recent comparison of results from the Nernst and Parsegian charge regulation boundary condition [Eqs. (1) and (2)] with those of Monte Carlo simulations for charge regulating surfaces demonstrates good agreement between the approaches for low surface densities, $\Gamma = 0.1/\text{nm}^2$ of ionizable groups, which is the upper limit of the range of interest in this work.⁴⁴ Moreover for reasons previously outlined, the use of an effective pK higher than the bulk value is likely to be required to correctly model experimental observations.

Having obtained the electrical potential distribution, we evaluate the electrostatic interaction energy using a combination of volume and surface integrals as described previously.^{27,42,43,45} Thus, we have

$$F_{\text{el}}(x) = - \int_V \left\{ \frac{\epsilon\epsilon_0}{2} \mathbf{E}(\mathbf{r}; x) \cdot \mathbf{E}(\mathbf{r}; x) + 2c_0 k_B T (\cosh \psi(\mathbf{r}; x) - 1) \right\} dV + \Gamma k_B T \int_S \ln \frac{1 - \alpha(\mathbf{R}; x)}{1 - \alpha(\mathbf{R}; \infty)} dA, \quad (4)$$

where $\mathbf{E}(\mathbf{r}; x)$ denotes the electric field at a point \mathbf{r} in the electrolyte for an interparticle surface separation, x . The interfacial term, $F_{\text{int}}(x)$ in Eq. (3) represents the contribution from the orientational behavior of the interfacial water molecules. This term is calculated based on the MD simulation results for the excess hydration free energy $f(\sigma)$ per unit area [Fig. 2(d)]. Owing to charge regulation, the charge density σ at any point of the particle surface is a function of the inter-surface separation x [Fig. 3(a)]. Thus, for a given value of x , the term F_{int} is calculated via the surface integral

$$F_{\text{int}}(x) = \int_S f(\sigma(\mathbf{R}; x)) dA. \quad (5)$$

Note that the assumption of free-energy additivity implicit in Eq. (3) has a long history. Dating back at least to the Derjaguin–Landau–Verwey–Overbeek (DLVO) theory, such assumptions are widely used in colloidal science in order to partition interaction free energies.^{46,47} In particular, concerning the summation of hydration and electrostatic forces, the assumption has been explicitly tested in atomistic simulations and found to hold within accuracy limits under the relevant conditions.³

V. ATTRACTION IN THE WEAKLY CHARGED NEGATIVE REGIME CAUSED BY THE INTERFACIAL FREE ENERGY COMPONENT

Figure 3 illustrates the proposed mechanism by which an attraction may manifest in the interaction of like-charged particles in solution. As two like-charged objects approach, regulation decreases the magnitude of their electrical charge [Figs. 3(a) and 3(c)], but the counterions in the gap, which are required to preserve electroneutrality, resist compression. Therefore, as long as the particles retain a net electrical charge, the overall electrostatic component of the interaction, ΔF_{el} —including both the field energy and configurational entropy of the ions—generally remains repulsive over the entire distance range.^{29,45}

But, according to the MD results, as well as independent spectroscopic confirmation, a reduction in surface charge density influences the average orientation of interfacial water and, therefore, alters the interfacial hydration free energy [Fig. 3(b)]. The MD

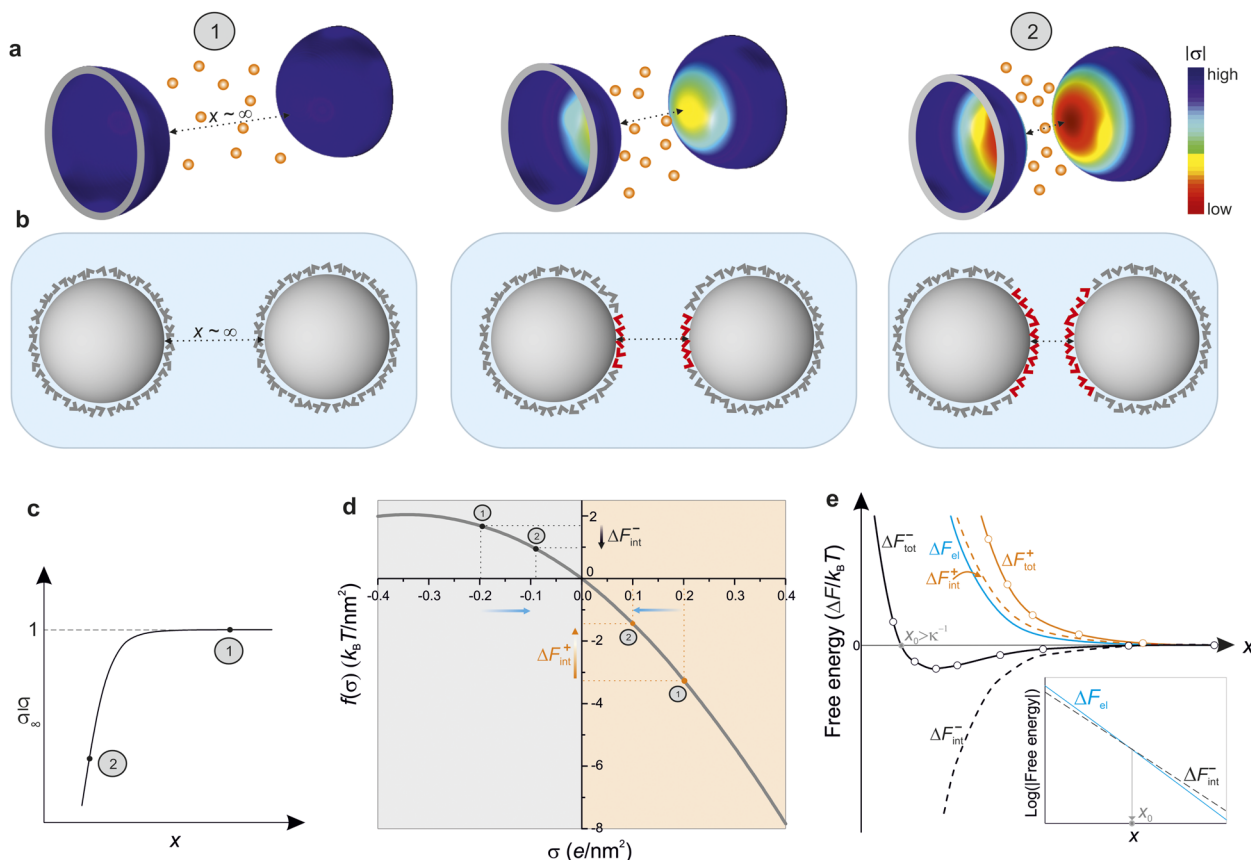


FIG. 3. Mechanism explaining the attraction between like-charged objects in solution. (a) As two like-charged particles approach each other from large separation (left to right), the charge density, σ , on the facing regions decreases in magnitude due to charge regulation. The counterions in the gap (orange spheres, not to scale) give rise to an entropic repulsion. (b) Since the orientation of the interfacial water molecules is a function of surface charge density [Figs. 1(b) and 2(b)], water molecules in the facing regions (colored red) respond to the local change of σ . The schematic depiction of water orientation is for weakly charged negative surfaces. (c) A schematic representation of the local charge density, σ relative to its value σ_∞ at infinite separation, as a function of x for points on the surface lying on the line connecting the particle centers. (d) Response of the interfacial free energy to a reduction in the magnitude of σ in the facing regions for both negative and positive particle charge. In the regime $|\sigma| < 0.3 \text{ e}/\text{nm}^2$, the reorientation of the interfacial water molecules results in a reduction of free energy for negative particles but an increase for positive particles. (e) The sum of the electrostatic free energy, ΔF_{el} (blue curve) and the water contribution ΔF_{int} (dashed black line) results in a total potential, ΔF_{tot} (solid black curve), which can go through a minimum at a very long range for the interaction of two negative particles, while it remains monotonically repulsive for the interaction of two positive particles (solid orange curve). The inset illustrates how the magnitude of the attractive interfacial contribution $|\Delta F_{\text{int}}^-|$ can dominate at a large interparticle separation, while the repulsive $|\Delta F_{\text{el}}|$ is dominant on closer approach. The case presented corresponds to conditions similar to that for curve viii in Fig. 4.

results suggest that in the weakly charged regime, $|\sigma| < 0.3 \text{ e}/\text{nm}^2$, an approach of two negative like-charged particles is accompanied by a reduction in the free energy of interfacial water, F_{int} owing to a down regulation of the surface charge [Fig. 3(d)]. This attractive interfacial contribution counteracts the increase in free energy due to electrostatic repulsion, F_{el} . In the regime of finite sized interacting spheres, given by say, $\kappa R \leq 50$, the attractive interfacial contribution can under certain conditions dominate the electrostatic repulsion and result in an interaction energy minimum in the potential of mean force at fairly long range ($x > \kappa^{-1}$) [Fig. 3(e), black curve]. Importantly, this model does not support an attraction for approaching positive particles, as here the hydration free energy of water increases monotonically with decreasing surface charge. This implies a

repulsive rather than an attractive interfacial contribution to the total free energy for approaching positive particles [Fig. 3(e), orange curves].

We remark that in practice it is challenging to obtain negatively charged surfaces with $|\sigma| \gg 0.3 \text{ e}/\text{nm}^2$ in electrolytes of $\text{pH} \leq 7$, particularly at low ionic strength ($c_0 < 1 \text{ mM}$) (supplementary material Fig. S1). Even at higher ionic strengths of ca. 100 mM and ionizable group densities $\Gamma > 0.3/\text{nm}^2$, the regime of $|\sigma| < 0.3 \text{ e}/\text{nm}^2$ is attained for pH values up to about one unit higher than the pK value. For $\Gamma < 0.3/\text{nm}^2$, however, $|\sigma|$ is always less than $0.3 \text{ e}/\text{nm}^2$, and an attractive solvation energy contribution could be relevant regardless of pH and ionic strength [supplementary material Fig. S1(c)]. This implies a potentially ubiquitous role for interfacial water in

generating an attractive interaction between weakly negatively charged objects in aqueous solution.

VI. COMPARING THE CALCULATED TOTAL INTERACTION FREEE ENERGY WITH EXPERIMENT

We now compare our calculations of the total free energy, $\Delta F_{\text{tot}}(x)$, with observations from two experimental studies in the literature. The first set of measurements concerns interparticle interaction potentials inferred from radial distribution functions, $g(r)$ for negatively charged polystyrene latex spheres of radius $R = 0.65 \mu\text{m}$ in low ionic strength solution measured by optical microscopy [Fig. 4(a)].¹⁰ The experimental conditions involved Debye screening lengths κ^{-1} of about 50–250 nm, and the measurements typically revealed long-range attraction interaction potentials with shallow minima located at interparticle separations between 0.5 μm and 2 μm [Figs. 4(b)–4(d), square symbols]. The electrolyte in the study was deionized water, which typically contains ions at a concentration $c_0 \approx 10 \mu\text{M}$ and has a pH of about 5.5 due to dissolution of CO_2 from ambient air [Fig. 4(b)].

Contact with deionizing resin in some measurements [Figs. 4(c) and 4(d)] reduces the ion concentration, c_0 by an order of magnitude

down to a value of about 1 μM , which corresponds approximately to a resistivity of 18 $\text{M}\Omega \text{ cm}$. It is fair to assume that this simultaneously returns the pH of the electrolyte to its neutral value of 7. Since the pH and ion concentration could not be measured directly in the experiments, we work with values of pH and c_0 estimated as described above.

The solid lines correspond to calculations of $\Delta F_{\text{tot}}(x)$ based on a nominal surface density of ionizable groups, $\Gamma = 0.1/\text{nm}^2$, in electrolytes of various ionic strengths. Given the uncertainty in the effective pK value of the surface sulfonate groups in Eq. (2), this quantity was treated as an adjustable parameter. Best agreement between experiment and calculation was obtained for pK values between 3 and 3.5. Although the pK of the isolated sulfonic acid group in free solution is about −0.5, measurements and calculations indeed suggest a value of about 3 for oligomers of styrenesulfonic acid.²⁵ Thus, the proximity of the low-dielectric particle interior,²⁵ altered solvation energy at an interface compared to the bulk,²⁸ and the inclusion of small amounts of carboxylic acid groups during the synthesis process may also contribute to a slightly increased effective pK . In the figure, calculated pair potentials are shown for various combinations of the parameter $p = z(\text{pH} - \text{pK})$ from −3.8 to −2 with corresponding c_0 values in the range 1–25 μM .

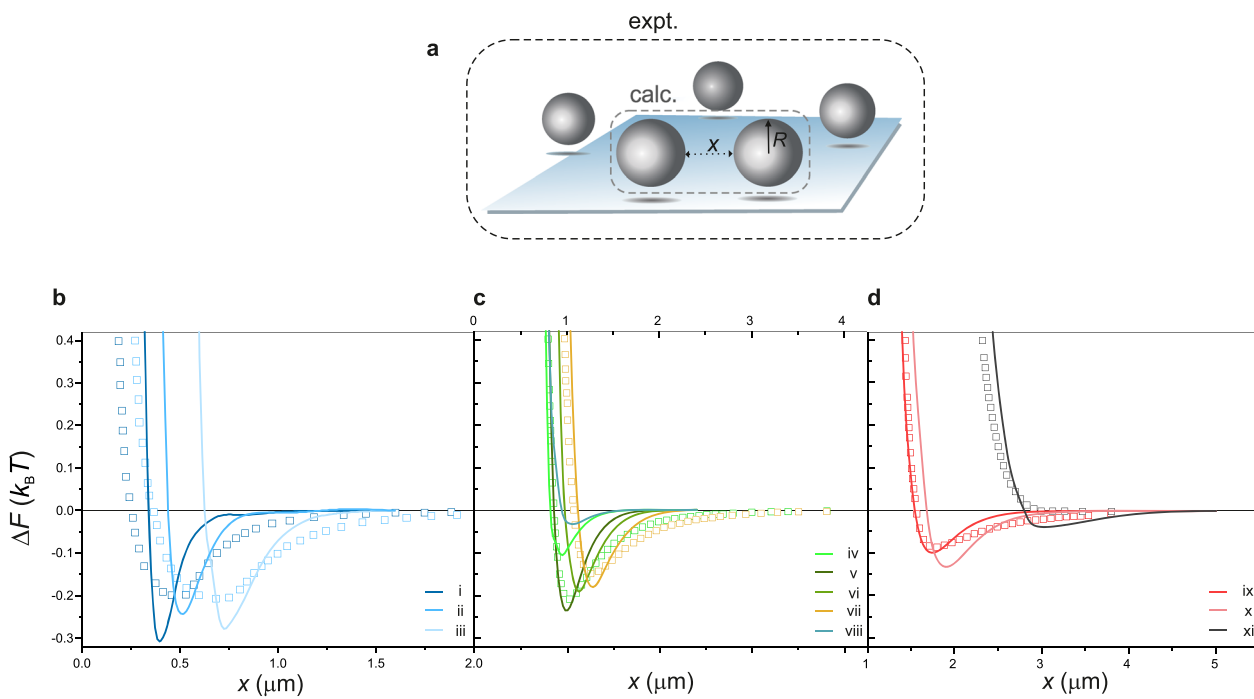


FIG. 4. Comparison of calculated interaction potentials with experimental data from Ref. 10. (a) Schematic depiction of the experimental situation where the diffusion of an ensemble of polystyrene colloidal particles of radius, $R = 0.65 \mu\text{m}$ is monitored above the surface of a glass coverslip by optical microscopy. (b)–(d) Pair potentials of the Lennard-Jones form inferred in Ref. 10 (square symbols), and our calculated potentials for $\Gamma = 0.1 \text{ nm}^{-2}$ (solid lines). Parameters for the calculated curves are quoted in the format $(p, c_0 \text{ in } \mu\text{M}, \kappa^{-1} \text{ in nm})$. (b) Measurements in deionized water with estimated κ^{-1} values of 62 nm (dark blue symbols) and 92 nm (light blue symbols). Parameters for the calculated curves are i: (−2, 16.6, 75), ii: (−2, 25, 61), and iii: (−2, 8.3, 106). (c) Measurements with deionizing resin achieving an intermediate ionic strength with estimated κ^{-1} values of 140 nm (green symbols) and 170 nm (yellow symbols). Parameters for the calculated curves are iv: (−2.1, 6.67, 118), v: (−2.05, 5, 136), vi: (−2.15, 4.17, 149), vii: (−2.15, 3.33, 167), and viii: (−2.2, 6.67, 118). (d) Measurements with deionizing resin achieving the lowest ionic strength with an estimated κ^{-1} value of 230 nm (red symbols), and an even larger value (black symbols). Parameters for the calculated curves are ix: (−2.4, 2.1, 210), x: (−2.45, 1.67, 235), and xi: (−3.8, 0.83, 334).

Considering the wide range of qualitatively different behaviors resulting from slightly different calculation parameters [e.g., Fig. 4(c)], it appears that the experimental observation could range from a nearly vanishing attraction to a minimum in the potential

of depth around $0.5 k_B T$. The calculations thus suggest that the presence of the well, and its depth, would be highly sensitive to the pH and the ionic strength; this is indeed in line with reports in the experimental literature.^{14,16,48,49} In practice, small drifts of

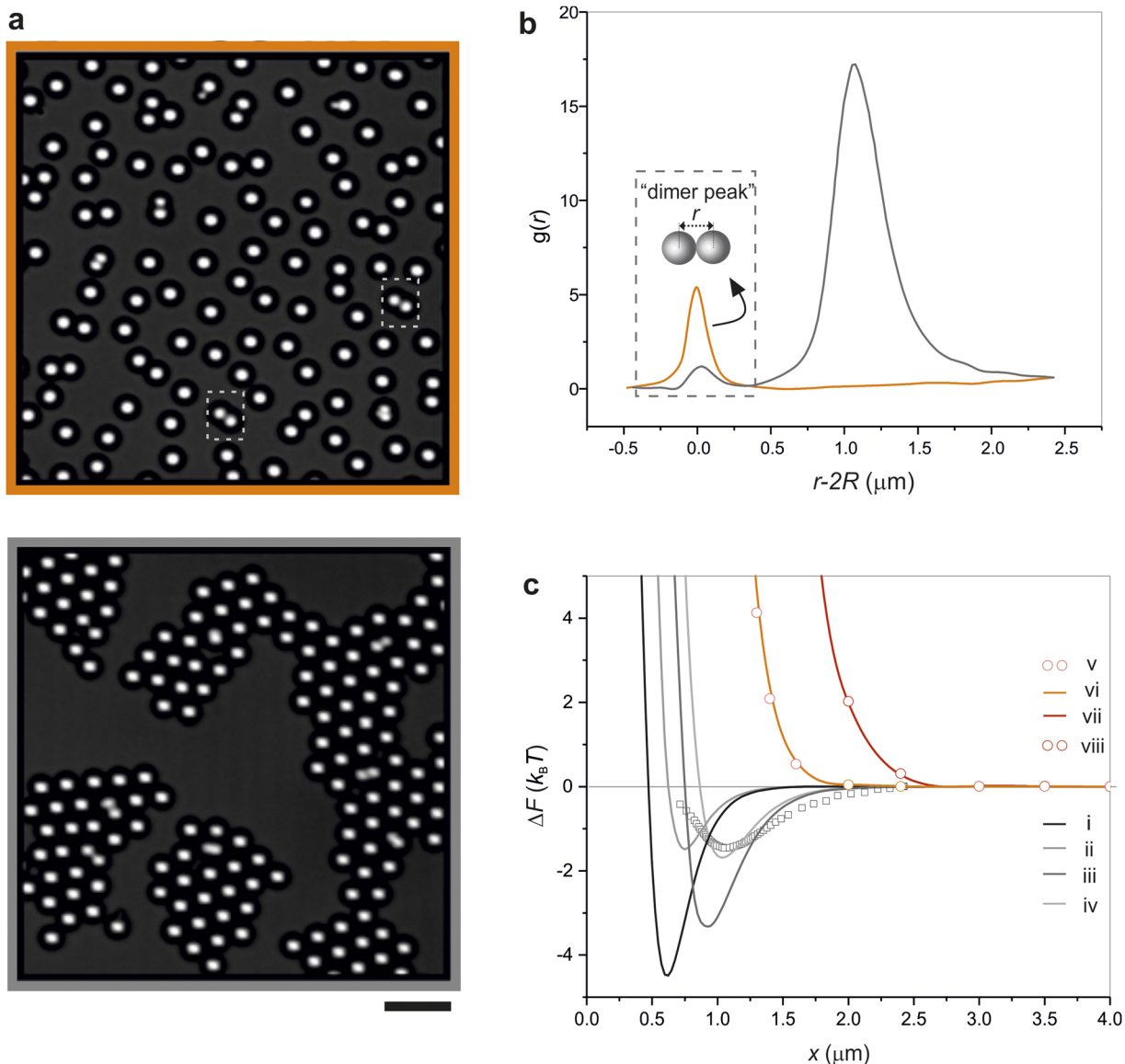


FIG. 5. Broken symmetry in the response of the pair potential to a change in the sign of the particle charge. (a) Optical microscopy snapshots of particles coated with positive lipid bilayers (top) and negative bilayers (bottom), indicating repulsive interactions in the former case and long range attractive interactions in the latter (images reproduced with permission from Ref. 18). Scale bar denotes $20 \mu\text{m}$. “Dimers” (demarcated in dashed boxes) are irreversibly aggregated pairs of particles inevitably present in colloidal preparations and irrelevant to the interpretation of long-range interparticle attractions of interest here. (b) Radial probability density distributions, $g(r)$ reported for the above cases, including only the first significant peak in $g(r)$ (Black curve - negative particles, orange curve—positive particles). (c) Calculated interaction potentials for $R = 3.25 \mu\text{m}$ particles (solid curves) with parameters presented in the format $(p, c_0 \text{ in } \mu\text{M}, \Gamma \text{ in } \text{nm}^{-2})$. Curves for negatively charged particles, i: $(-2.3, 4.17, 0.01)$, ii: $(-2.1, 4.17, 0.025)$, iii: $(-2.28, 2.1, 0.01)$, and iv: $(-2, 2.1, 0.025)$. Curves for positively charged particles, v: $(-4.5, 4.17, 0.035)$, vi: $(-4.5, 4.17, 0.055)$, vii: $(-4.5, 2.08, 0.035)$, and viii: $(-4.5, 2.08, 0.055)$. Salt concentrations, $c_0 \approx 2\text{--}4 \mu\text{M}$ used in the calculations are comparable to the reported experimental value of $c_0 \sim 5 \mu\text{M}$ for deionized water equilibrated with air. In the absence of a measured pair potential, $-k_B T \ln g(r)$ is reported as a crude estimate [square symbols, based on the black curve in panel (b)] of the range and depth of the attractive minimum for the experiments on negative particles.

conductivity and pH during the measurements, variability in the particle size R , and ionizable group density Γ , along with the out-of-plane (vertical) motion of the particles, are all expected to smear out the measured response,¹⁰ thereby causing unavoidable discrepancies between experiment and calculation. In particular, the functional form of the measured pair potentials at close approach ($x < 0.5 \mu\text{m}$) could be particularly sensitive to uncertainties in particle size on the order of $0.1 \mu\text{m}$. Nevertheless, we obtain remarkable agreement between calculated and experimental curves for plausible values of the system parameters.

VII. INTERFACIAL HYDRATION EXPLAINS SYMMETRY-BREAKING BEHAVIOR IN THE INTERACTION BETWEEN LIKE-CHARGED PARTICLES

The second set of experimental observations concerns reports of Groves *et al.*, which extend the observation of like-charge attraction to much larger micron-scale silica particles, $R = 3.25 \mu\text{m}$, coated with lipid bilayers composed of a mixture of charged and uncharged lipids with tunable composition.^{15,18} Here, the observed long-range interparticle attraction is so strong that it results in stable clusters of hexagonally close-packed particles [Fig. 5(a), bottom panel], implying an attractive minimum in the pair potential whose depth is at least an order of magnitude larger than that inferred in the polystyrene latex sphere experiments.^{10,49} Again, as previously reported, the attractive minima as inferred from the measured radial distribution functions occur at intersurface separations of several hundreds of nanometers [Fig. 5(b)]. However, very intriguingly, this study reported attractions only for negatively charged particles and not for particles coated with net positively charged lipid bilayers [Fig. 5(a), top panel].

The experiments were performed using mole fractions of charged lipids of 1%–5% for the negative lipids and 7%–11% for the positive case. Assuming an area per lipid head group of 2 nm^2 , the ionizable group densities probed correspond to ranges in Γ of $0.005\text{--}0.025 \text{ nm}^{-2}$ and $0.035\text{--}0.055 \text{ nm}^{-2}$ for experiments with negative and positive lipids, respectively. Calculations of $\Delta F_{\text{tot}}(x)$ reveal deep minima of about $1\text{--}4 k_B T$ at experimentally reported interparticle distances of around $1 \mu\text{m}$ for the negatively charged system [Fig. 5(c), curves i–iv]. Given that the pH of water exposed to air is about 5.5 to 6, the values of p in the calculated curves imply pK values of 3.2–3.9, which are in excellent agreement with the reported pK values of lipid head groups in the negatively charged lipid bilayers used in the experimental study.⁵⁰ The significantly larger well depths in these experiments with $R = 3.25 \mu\text{m}$ compared with the polystyrene experiments, where $R = 0.65 \mu\text{m}$ (Fig. 4) are consistent with an attractive contribution growing approximately in proportion to the particle surface area (ratio of areas = 25). Such scaling is to be expected for an effect mediated by interfacial water molecules [Fig. 3(b)].

Calculations were also performed for positively charged particles assuming basic ionizable surface groups with pK = 10, giving $p = \text{pH} - \text{pK} = -4.5$. In this case, the interaction remains monotonically repulsive, indicating the absence of cluster formation, which is consistent with the experimental observations [Fig. 5(c), curves v–viii].

VIII. CONCLUSIONS

In conclusion, our findings provide a plausible mechanism for the observed attraction of like-charged objects in aqueous solution. Rather than pointing to a failure of mean-field theory, the experimental observations indicate the need for additional molecular level information absent in continuum theories: more specifically, the orientation of interfacial solvent molecules as shown in this study. While the framework of classical electromagnetics, and possible corrections from, e.g., fluctuation forces²⁰ or charge inversion,⁵¹ would not support a symmetry broken response to complete inversion of the sign of charge in the system, the proposed interfacial mechanism unambiguously does. While errors in image processing can in some experiments lead to a spurious shallow minimum ($<0.5 k_B T$) in an otherwise repulsive interaction potential,^{16,23,52} the deep minima ($\sim 5 k_B T$) observed in the work of Groves *et al.* and similar studies⁵³ cannot be ascribed to such artifacts.

Although the present study focuses on explaining experimental observations in low ionic strength solution, the scaling of the screened electrostatic interaction implies that the same considerations hold at much higher ionic strengths and at correspondingly closer distances of approach between the interacting objects. In particular, the proposed mechanism may be capable of explaining a pH-tunable affinity between negatively charged macromolecules that is repulsive at higher pH and turns attractive under more acidic conditions even though the molecules carry substantial net negative charge over the entire pH range of interest.⁵⁴ This behavior is distinct from the fluctuation induced attraction anticipated for molecules close to their isoelectric points (or point of zero charge),^{55,56} and may be relevant in a broad range of phenomena, such as biological phase segregation,⁵⁴ crystallization,⁵⁷ histone-bound packaging of DNA in the nucleus, formation and dissolution of polyphosphate stress granules,⁵⁸ phosphorylation-based modulation of molecular interactions, or, indeed more generally, in any system involving interactions between or with entities of low net negative charge density. It is worth noting that the pH range of interest in this study, 5.5–7, is similar to that associated with the formation and dissolution of biomolecular condensates and intracellular phase separation in biological organisms,^{54,59} where the relevant charged groups have pKs of about 4, similar to the colloidal particles considered in our study. Although the results presented at this stage for comparatively macroscopic objects would not warrant quantitative predictions on interactions at the molecular scale, the generality of the mechanism raises the distinct possibility of relevance in this context. Furthermore, chemical details of the surface may play an important role, especially in complex materials such as zwitterionic lipids and oxides like silica composed of different species of ionizable groups with widely different pKs and hydrogen-bonding capability. Importantly, however, our findings based on MD simulations involving non-polar and non-hydrogen-bonding walls suggest that the chemical nature of the surface is likely to play a role subordinate to its electrical charge. Although our minimal model of surface–water interactions should not be expected to provide a quantitative description of interactions in all systems, it is remarkable that this simplified picture is capable of explaining hitherto unexplained observations in remarkable detail. Future experiments aim at performing further rigorous tests of the predictions of this

model and refinements thereof. Our findings could point to a new fundamental understanding of the contribution of molecular water in interparticle and intermolecular interactions in solution.

SUPPLEMENTARY MATERIAL

Supplementary material accompanies this manuscript and provides additional information on the MD simulations as well as plots of surface charge density as a function of various quantities of interest.

ACKNOWLEDGMENTS

P.H.H. gratefully acknowledges financial support from the Swiss National Science Foundation (Grant No. 200021-175944). M.K. gratefully acknowledges the European Research Council for financial support.

REFERENCES

- ¹M. M. Reif and P. H. Hunenberger, *J. Phys. Chem. B* **120**(33), 8485–8517 (2016).
- ²S. I. Mamakulov, C. Allolio, R. R. Netz, and D. J. Bonthuis, *Angew. Chem., Int. Ed.* **56**(50), 15846–15851 (2017).
- ³A. Schlaich, A. P. dos Santos, and R. R. Netz, *Langmuir* **35**(2), 551–560 (2019).
- ⁴W. Kung, P. Gonzalez-Mozuelos, and M. O. de la Cruz, *Soft Matter* **6**(2), 331–341 (2010).
- ⁵J. E. Sader and D. Y. C. Chan, *J. Colloid Interface Sci.* **213**(1), 268–269 (1999).
- ⁶J. C. Neu, *Phys. Rev. Lett.* **82**(5), 1072–1074 (1999).
- ⁷W. A. P. Luck and I. Stranski, *Phys. Bl* **23**(8), 10 (1967).
- ⁸A. Kose, M. Ozaki, K. Takano, Y. Kobayash, and S. Hachisu, *J. Colloid Interface Sci.* **44**(2), 330–338 (1973).
- ⁹R. Williams, R. S. Crandall, and P. J. Wojtowicz, *Phys. Rev. Lett.* **37**(6), 348–351 (1976).
- ¹⁰G. M. Kepler and S. Fraden, *Phys. Rev. Lett.* **73**(2), 356–359 (1994).
- ¹¹D. G. Grier, *Nature* **393**(6686), 621–623 (1998).
- ¹²A. E. Larsen and D. G. Grier, *Nature* **385**(6613), 230–233 (1997).
- ¹³D. G. Grier, *J. Phys.-Condens. Matter* **12**(8A), A85–A94 (2000).
- ¹⁴Y. L. Han and D. G. Grier, *Phys. Rev. Lett.* **91**(3), 038302 (2003).
- ¹⁵M. M. Baksh, M. Jaros, and J. T. Groves, *Nature* **427**(6970), 139–141 (2004).
- ¹⁶M. Polin, D. G. Grier, and Y. Han, *Phys. Rev. E* **76**(4), 041406 (2007).
- ¹⁷M. Krishnan, I. Monch, and P. Schwille, *Nano Lett.* **7**(5), 1270–1275 (2007).
- ¹⁸E. W. Gomez, N. G. Clack, H. J. Wu, and J. T. Groves, *Soft Matter* **5**(9), 1931–1936 (2009).
- ¹⁹M. U. Musheev, M. Kanoatov, C. Retif, and S. N. Krylov, *Anal. Chem.* **85**(21), 10004–10007 (2013).
- ²⁰M. Kardar and R. Golestanian, *Rev. Mod. Phys.* **71**(4), 1233–1245 (1999).
- ²¹E. Trizac and J. L. Raimbault, *Phys. Rev. E* **60**(6), 6530–6533 (1999).
- ²²L. Belloni, *J. Phys.-Condens. Matter* **12**(46), R549–R587 (2000).
- ²³J. Baumgartl and C. Bechinger, *Europhys. Lett.* **71**(3), 487–493 (2005).
- ²⁴A. P. dos Santos and Y. Levin, *Phys. Rev. Lett.* **122**(24), 248005 (2019).
- ²⁵H. T. Dong, H. B. Du, S. R. Wickramasinghe, and X. H. Qian, *J. Phys. Chem. B* **113**(43), 14094–14101 (2009).
- ²⁶B. W. Ninham and V. A. Parsegian, *J. Theor. Biol.* **31**(3), 405–428 (1971).
- ²⁷P. M. Biesheuvel, *J. Colloid Interface Sci.* **275**(2), 514–522 (2004).
- ²⁸P. Loche, C. Ayaz, A. Schlaich, D. J. Bonthuis, and R. R. Netz, *J. Phys. Chem. Lett.* **9**(22), 6463–6468 (2018).
- ²⁹R. Pericet-Camara, G. Papastavrou, S. H. Behrens, and M. Borkovec, *J. Phys. Chem. B* **108**(50), 19467–19475 (2004).
- ³⁰I. Popa, P. Sinha, M. Finessi, P. Maroni, G. Papastavrou, and M. Borkovec, *Phys. Rev. Lett.* **104**(22), 228301 (2010).
- ³¹P. Jedlovszky and M. Mezei, *J. Phys. Chem. B* **105**(17), 3614–3623 (2001).
- ³²M. P. Gaigeot, M. Sprak, and M. Sulpizi, *J. Phys.-Condens. Matter* **24**(12), 124106 (2012).
- ³³Y. R. Shen and V. Ostroverkhov, *Chem. Rev.* **106**(4), 1140–1154 (2006).
- ³⁴S. W. Ong, X. L. Zhao, and K. B. Eisenthal, *Chem. Phys. Lett.* **191**(3–4), 327–335 (1992).
- ³⁵M. S. Yeganeh, S. M. Dougal, and H. S. Pink, *Phys. Rev. Lett.* **83**(6), 1179–1182 (1999).
- ³⁶J. A. Mondal, S. Nihonyanagi, S. Yamaguchi, and T. Tahara, *J. Am. Chem. Soc.* **132**(31), 10656–10657 (2010).
- ³⁷A. Myalitsin, S. H. Urashirna, S. Nihonyanagi, S. Yamaguchi, and T. Tahara, *J. Phys. Chem. C* **120**(17), 9357–9363 (2016).
- ³⁸C. Macias-Romero, I. Nahalka, H. I. Okur, and S. Roke, *Science* **357**(6353), 784–787 (2017).
- ³⁹Q. Du, E. Freysz, and Y. R. Shen, *Phys. Rev. Lett.* **72**(2), 238–241 (1994).
- ⁴⁰S. Ye, S. Nihonyanagi, and K. Uosaki, *Phys. Chem. Chem. Phys.* **3**(16), 3463–3469 (2001).
- ⁴¹V. Ostroverkhov, G. A. Waychunas, and Y. R. Shen, *Phys. Rev. Lett.* **94**(4), 046102 (2005).
- ⁴²M. Krishnan, *J. Chem. Phys.* **138**(11), 114906 (2013).
- ⁴³M. Krishnan, *J. Chem. Phys.* **146**(20), 205101 (2017).
- ⁴⁴A. Bakhshandeh, D. Frydel, A. Diehl, and Y. Levin, *Phys. Rev. Lett.* **123**(20), 208004 (2019).
- ⁴⁵J. T. G. Overbeek, *Colloids Surf.* **51**, 61–75 (1990).
- ⁴⁶E. J. W. Verwey and J. T. G. Overbeek, *Theory of the Stability of Lyophobic Colloids* (Elsevier, Amsterdam, 1948).
- ⁴⁷V. A. Parsegian, R. P. Rand, and N. L. Fuller, *J. Phys. Chem.* **95**(12), 4777–4782 (1991).
- ⁴⁸J. C. Crocker and D. G. Grier, *Phys. Rev. Lett.* **77**(9), 1897–1900 (1996).
- ⁴⁹D. G. Grier and Y. Han, *J. Phys.-Condens. Matter* **16**(38), S4145–S4157 (2004).
- ⁵⁰F. C. Tsui, D. M. Ojcius, and W. L. Hubbell, *Biophys. J.* **49**(2), 459–468 (1986).
- ⁵¹M. D. Carbajal-Tinoco and P. Gonzalez-Mozuelos, *J. Chem. Phys.* **117**(5), 2344–2350 (2002).
- ⁵²J. Baumgartl, J. L. Arauz-Lara, and C. Bechinger, *Soft Matter* **2**(8), 631–635 (2006).
- ⁵³P.-K. Lin, K.-h. Lin, C.-C. Fu, K.-C. Lee, P.-K. Wei, W.-W. Pai, P.-H. Tsao, Y.-L. Chen, and W. S. Fann, *Macromolecules* **42**, 1770–1774 (2009).
- ⁵⁴T. M. Franzmann, M. Jahnel, A. Pozniakovskiy, J. Mahamid, A. S. Holehouse, E. Nuske, D. Richter, W. Baumeister, S. W. Grill, R. V. Pappu, A. A. Hyman, and S. Alberti, *Science* **359**(6371), eaao5654 (2018).
- ⁵⁵J. G. Kirkwood and J. B. Shumaker, *Proc. Natl. Acad. Sci. U. S. A.* **38**(10), 863–871 (1952).
- ⁵⁶M. Lund and B. Jonsson, *Q. Rev. Biophys.* **46**(3), 265–281 (2013).
- ⁵⁷A. Klug, R. E. Franklin, and S. P. F. Humphreysowen, *Biochim. Biophys. Acta* **32**(1), 203–219 (1959).
- ⁵⁸J. W. McGrath and J. P. Quinn, *Appl. Environ. Microbiol.* **66**(9), 4068–4073 (2000).
- ⁵⁹S. Maharana, J. Wang, D. K. Papadopoulos, D. Richter, A. Pozniakovskiy, I. Poser, M. Bickle, S. Rizk, J. Guillen-Boixet, T. M. Franzmann, M. Jahnel, L. Marrone, Y. T. Chang, J. Sterneckert, P. Tomancak, A. A. Hyman, and S. Alberti, *Science* **360**(6391), 918–921 (2018).